A New Analysis of Internal Cation Mobilities in the Molten Binary System (Li, K)Cl†

Isao Okada,*,‡ Hiroshi Horinouchi,§ and Frédéric Lantelme‖

Department of Chemistry, Faculty of Science and Engineering, Sophia University, Kioi-cho 7-1, Chiyoda-ku, Tokyo 102-8554, Japan, Department of Electronic Chemistry, Tokyo Institute of Technology, Nagatsuta 4259, Midori-ku, Yokohama 226-8554, Japan, and Laboratoire LI2C, Université Pierre et Marie Curie, 4 Place Jussieu 75252 Paris Cedex 05, France

Internal mobilities of Li^+ and K^+ in the molten binary system (Li, K)Cl have been measured at (913 and 973) K. The product of the internal mobility and the modified molar volume has a constant value for Li^+ at 913 K and two constant values depending on concentration for Li^+ at 973 K and for K^+ at 913 K and at 973 K; the modified molar volume is the molar volume minus the deviation volume, appearing in an empirical equation previously presented. The present result is compared with that obtained for molten (Li, K)Br, which has previously been found to show a regular mode for the mobilities. The mobilities in the present system are attributable to the regular mode and, in addition, to the perturbed mode when the product has two values. The results are accounted for in terms of the dynamic dissociation model.

1. Introduction

Chemla[1] discovered the Chemla effect more than 50 years ago; he submitted a French patent in 1958, in which he claimed that in countercurrent electromigration (the Klemm method[2]) of the binary mixture of molten (Li, K)Br, the molar ratio of Li/K attains to a limited value at the anode, whereas the isotope ratio (^{7}Li/^{6}Li) (and also (^{41}K/^{39}K)) continues to increase with time. It was found later that this strange behavior is caused by the crossing of the isotherms of the mobilities of Li^+ and K^+ as a function of the mole fraction in the (Li, K)Br mixture.[3−7] At a higher concentration of LiBr, Li^+ is more mobile, and at a lower concentration of LiBr, K^+ is more mobile. That is, the more enriched cation than at the crossing-point concentration migrates faster in the anode compartment, where the ratio of the two cations, therefore, attains to that at the crossing point. This crossing phenomenon was later named the Chemla effect.[8] The Chemla effect can be the key for the elucidation of the mechanism of electrical conductivity in molten salts.

By an analysis of the original data presented by Chemla's group,[5−7] this binary system (Li, K)Br has been found to be an "ideal system"[9,10] in the following sense: The C_{IM}'s, defined by $C_{IM} = u_M(V_m - V_{0M})$, are constant practically over the whole investigated concentration range at a given temperature; M^+ is Li^+, K^+, and even Na^+ (which is contained as a trace amount of the radioisotope ^{22}Na), u_M the internal mobility of the cation M^+ (i.e., the cation mobility with reference to the common anion, Br^-), V_m the molar volume, and V_{0M} a correction factor characteristic of M^+.

The internal mobilities in the molten binary system (Li, K)Cl have been studied in the present work in comparison with those in the system (Li, K)Br. This will also help in the elucidation of the mechanism of ionic conductivities in simple molten salts such as alkali chloride and bromide melts. Data on the mobilities in binary systems with a common anion can supply us with much more information concerning the mechanism[11−14] than those in pure melts such as LiCl.

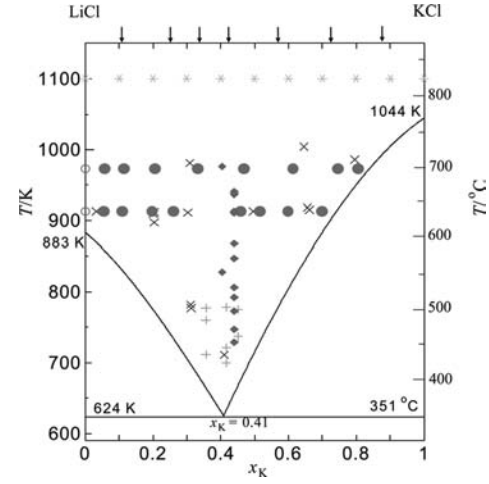

Figure 1. Points on the phase diagram of (Li, K)Cl where the internal mobilities have been measured. ●, this work; ○, pure LiCl; ×, Moynihan and Laity;[16] ∗, Smirnov et al.;[17] +, Takagi et al.;[18] ◆, Lundén and Okada.[19] The mark ↓ indicates the concentrations where the equations of the conductivities, κ, are given as a function of temperature.[15]

In the binary system (Li, K)Cl, the internal mobilities have so far been measured by several groups. The mole fractions and the temperatures where the data are obtained in the present study are given in Figure 1 on the phase diagram,[15] together with those in previous studies.[16−19]

2. Experimental Section

Reagent grade LiCl and KCl, made by the Wako Co. Ltd., were vacuum-dried at 423 K for 2 days. The melts to be used in the separation tube were bubbled with dried argon for a few hours and not dehydrated further, since, with the Klemm method, the measured values of the relative difference in internal

† Part of the "Josef M. G. Barthel Festschrift".

* Corresponding author. Tel.: +81-3-5357-8205. Fax: +81-3-5357-8205. E-mail: i-okada@dol.hi-ho.ne.jp.
‡ Sophia University.
§ Tokyo Institute of Technology. E-mail: isac_okada@hotmail.com.
‖ Université Pierre et Marie Curie. E-mail: frederic.lantelme@upmc.fr.

10.1021/je900866q
Published on Web 03/04/2010

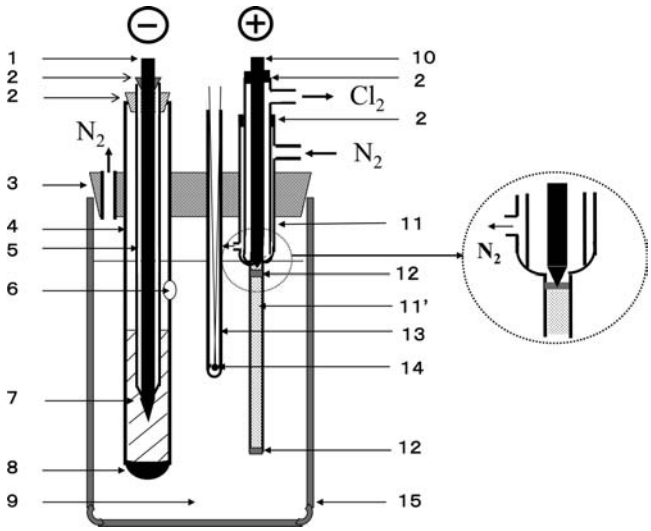

Figure 2. Electromigration cell. In the inset, the anode part is enlarged. 1, graphite cathode; 2, silicone stopper; 3, graphite lid; 4, alumina tube; 5, alumina tube; 6, alumina wool; 7, $PbCl_2$ melt; 8, electrolyzed Pb melt; 9, (Li, Na, K)Cl at about the eutectic composition; 10, graphite anode; 11, separation tube of Vycor glass; 11′, diaphragm part (int. diam.: 4 mm, length: ca. 200 mm) of the separation tube; 12, alumina wool; 13, alumina sheath; 14, thermocouple; 15, Tammann tube of alumina (int. diam.: 42 mm, ext. diam.: 50 mm, length: 350 mm).

mobilities ε (defined in Section 3, Results) are insensitive to small amounts of impurities or moisture.[20]

The melt, contained in a small vessel, was quickly filled into the separation tube by vacuum suction so as to avoid a chemical fractionation during the filling.

To cover a wider temperature range, we used a mixture of the eutectic composition (Li, Na, K)Cl [(53.5, 8.6, 37.9) % (by mol); m.p.: 619 K] as a thermostat bath in the large compartment.

In the anode compartment, molten $PbCl_2$ was used, which was electrolyzed into a Pb melt precipitated there. This process avoids the troublesome bubbling of chlorine gas into the cathode compartment.

After introduction of the separation tube into the large container, electromigration was started immediately. One serious problem was the creeping of the melt along the vessel walls. To prevent this, we flowed dried nitrogen gas at room temperature into the vessel so as to cool the part shown in Figure 2. This will not affect the validity of the equation for the calculation of ε, because this equation[21] is based only on the material balance and the transported charge balance through a plane in the separation tube where the initial composition is kept constant during electromigration. The temperature was kept constant there and measured by a thermocouple set nearby.

Electromigration was performed for (2 to 4) h under a constant electric current [(250 to 350) mA], and the voltage was (40 to 120) V. After electromigration, the separation tube was cut into several sections of about 1 cm, and the contents of Li^+ and K^+ were determined by flame spectrophotometry.

Further details of the experimental method were previously given in ref 22.

3. Results

Internal mobilities are calculated from the measured ε values from eqs 1 and 2:

$$u_{Li} = (\kappa V_m/F)(1 + x_K\varepsilon) \quad (1)$$

$$u_K = (\kappa V_m/F)(1 - x_{Li}\varepsilon) \quad (2)$$

where κ is the conductivity, V_m is the molar volume, x_M is the mole fraction of the cation M^+ ($x_{Li} + x_K = 1$), F is the Faraday constant, and ε is the relative internal mobility difference: $\varepsilon \equiv (u_{Li} - u_K)/(x_{Li}u_{Li} + x_Ku_K)$.

The values obtained for ε are given in Table 1 together with the main experimental conditions. The internal cation mobilities were calculated[21] from the ε values and the available data on the densities and conductivities.[15,23,24]

Table 1. Relative Difference, ε, in the Internal Mobilities, u, and Transported Charge, Q_t[a]

x_K	Q_t / C	ε	κ / $S\cdot m^{-1}$	$10^6\ V_m$ / $m^3\cdot mol^{-1}$	$10^7\ u_{Li}$ / $m^2\cdot V^{-1}\cdot s^{-1}$	$10^7\ u_K$ / $m^2\cdot V^{-1}\cdot s^{-1}$
			(a) $T = 913$ K			
0			5.844	28.47	1.724	
0.053	3927	0.099 ± 0.003	4.947	29.43	1.517 ± 0.001	1.367 ± 0.004
0.057	4138	0.092 ± 0.002	4.893	29.50	1.504 ± 0.001	1.366 ± 0.003
0.103	3866	0.056 ± 0.002	4.359	30.33	1.378 ± 0.001	1.301 ± 0.002
0.108	2049	0.052 ± 0.001	4.309	30.42	1.366 ± 0.001	1.295 ± 0.001
0.181	2008	0.032 ± 0.000	3.719	31.73	1.230 ± 0.000	1.191 ± 0.000
0.263	2631	−0.064 ± 0.001	3.184	33.21	1.078 ± 0.001	1.148 ± 0.001
0.358	2067	−0.118 ± 0.002	2.756	34.92	0.955 ± 0.001	1.073 ± 0.001
0.481	2240	−0.175 ± 0.001	2.362	37.14	0.832 ± 0.001	0.991 ± 0.001
0.536	1634	−0.193 ± 0.000	2.226	38.13	0.788 ± 0.000	0.958 ± 0.000
0.643	1631	−0.229 ± 0.001	2.022	40.05	0.716 ± 0.001	0.908 ± 0.001
0.656	2217	−0.230 ± 0.000	2.002	40.28	0.710 ± 0.000	0.902 ± 0.000
1			1.747	46.49		0.842
			(b) $T = 973$ K			
0			6.177	28.98	1.855	
0.053	3933	0.060 ± 0.004	5.313	29.96	1.637 ± 0.001	1.539 ± 0.006
0.097	3285	0.038 ± 0.004	4.740	30.78	1.507 ± 0.001	1.450 ± 0.005
0.213	2225	−0.038 ± 0.002	3.649	33.04	1.241 ± 0.001	1.289 ± 0.002
0.307	2253	−0.099 ± 0.001	3.138	34.67	1.085 ± 0.001	1.195 ± 0.001
0.397	1988	−0.129 ± 0.000	2.841	36.34	1.012 ± 0.000	1.149 ± 0.000
0.455	1803	−0.189 ± 0.001	2.678	37.42	0.949 ± 0.001	1.145 ± 0.001
0.568	1770	−0.214 ± 0.001	2.409	39.51	0.864 ± 0.001	1.075 ± 0.001
0.635	1782	−0.240 ± 0.002	2.273	40.76	0.816 ± 0.001	1.047 ± 0.001
0.762	1736	−0.271 ± 0.000	2.075	43.11	0.743 ± 0.000	0.996 ± 0.000
1			1.948	47.53		0.944

[a] The sign ± refers to the standard deviation originating only from the chemical analysis.

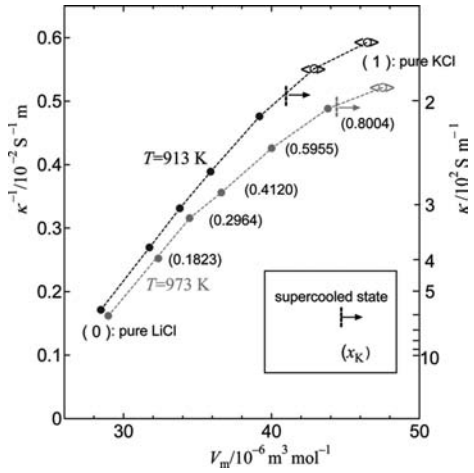

Figure 3. Reciprocal conductivities of (Li, K)Cl vs molar volume.[15] -<○>-, extrapolated value with respect to temperature for the imaginary supercooled melt.

The molar volumes of the mixtures were calculated from those of pure LiCl and KCl on the assumption of additivity; the excess molar volume is practically insignificant.[25] For example, the molar volume at $x_K = 0.4120$ at 973 K is 36.70 $cm^3 \cdot mol^{-1}$ according to established data,[15] while the value estimated from the additivity of pure LiCl and KCl is 36.62 $cm^3 \cdot mol^{-1}$,[24] and therefore the excess molar volume is only 0.22 %. When the melting points of the pure salts are above those of the melt mixtures, the molar volumes of the assumed "supercooled" melts of the pure salts (LiCl and KCl) are estimated by extrapolation with respect to temperature.

The electrical conductivities in the mixture systems at several concentrations have previously been measured. The ones at the concentrations measured in the present experiment are interpolated on the assumption of the "series model" presented by Fellner.[26] According to this model, the conductivity of the binary mixture, κ_m, can be expressed by those of the two pure melts, κ_{Li} and κ_K:[27]

$$(1/\kappa_m) = (1/\kappa_{Li})[x_{Li}V_{Li}^0/(x_{Li}V_{Li}^0 + x_KV_K^0)] + (1/\kappa_K)[x_KV_K^0/(x_{Li}V_{Li}^0 + x_KV_K^0)] \quad (3)$$

where $x_iV_i^0/(x_{Li}V_{Li}^0 + x_KV_K^0)$ is the molar volume fraction of LiCl and KCl; i = Li and K, respectively.

In Figure 3 the reciprocal conductivities, $1/\kappa$, obtained experimentally at several concentrations[15,23] are plotted against the molar volume at (913 and 973) K. The values near $x_K = 1$ are the ones corresponding to imaginary supercooled melts. For pure KCl($x_K = 1$), for example, the values are calculated from a quadratic equation: $\kappa/S \cdot cm^{-1} = -5.5231 + 1.1714 \cdot 10^{-2}(T/K) - 4.1800 \cdot 10^{-6}(T/K)^2$ [15] which has been fitted to the experimentally obtained values above 1070 K.

Figure 3 reveals that the series model holds well in the partial ranges of the molar volume, although it does not hold well over the whole range. Therefore, κ_m at a given molar volume is calculated by interpolation, using eq 3, from those of the two nearest experimentally obtained points.

The advantage of this method is that, as the series model holds well particularly at high x_{Li}, where κ changes sharply with concentration, κ at a given x_K can be unambiguously evaluated and, presumably, more accurately estimated than by using a spline curve for κ itself.

The isotherms of the internal mobilities calculated from eqs 1 and 2 at (913 and 973) K are shown in Figure 4. The Chemla

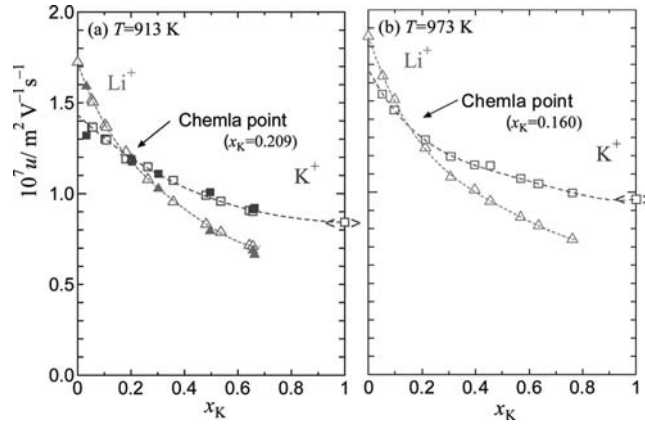

Figure 4. Isotherms of the internal mobilities at 913 K (a) and 973 K (b). △, □, Li^+ and K^+, respectively, this work; ▲, ■, Moynihan and Laity;[16] <□>, extrapolated for pure KCl with respect to temperature.

effect occurs, as was seen previously, at higher composition of KCl. There, the mobility of K^+ is greater than that of Li^+, and the Chemla (crossing) point occurs. The mole fractions x_K of the Chemla point are 0.209 and 0.160 at (913 and 973) K, respectively.

With increasing temperature, the Chemla point shifts toward higher concentrations of Li^+, that is, the smaller cation. The reason for this general trend has been previously stated.[11] The molar volumes of the Chemla point are 32.2 $cm^3 \cdot mol^{-1}$ (x_K = 0.209) and 32.0 $cm^3 \cdot mol^{-1}$ ($x_K = 0.160$) at (913 and 973) K, respectively; the difference happens to be negligibly small.

4. Discussion

4.1. Comparison with Previous Data on the Mobilities. Moynihan and Laity[16] measured the internal mobilities of Li^+ and K^+ by the Hittorf method. They measured the percent mobility difference, Q, defined as

$$Q \equiv 100(u_K - u_{Li})/u_{Li} \quad (4)$$

It follows from eq 4,

$$u_{Li} = (\kappa V_m/F)[1/(1 + x_K(Q/100))] \quad (5)$$

$$u_K = (\kappa V_m/F)[(1 + (Q/100))/(1 + x_K(Q/100))] \quad (6)$$

If it is assumed that the errors in u_{Li} and u_K come only from those in Q, the errors can be evaluated by

$$\sigma_{uLi} = |(\partial u_{Li}/\partial Q)\sigma_Q| = (\kappa V_m/F)[x_K/(1 + x_K(Q/100))^2](\sigma_Q/100) \quad (7)$$

$$\sigma_{uK} = |(\partial u_K/\partial Q)\sigma_Q| = (\kappa V_m/F)[(1 - x_K)/(1 + x_K(Q/100))^2](\sigma_Q/100) \quad (8)$$

These authors have obtained values of Q at 14 points of temperature and concentration, 7 points of which are at the values at about 913 K (640 °C). For comparison with the present data, the u_{Li} and u_K values at these 7 points are calculated from the Q values and given in Table 2. The values of κ and V_m are evaluated in the same way as in the present data.

The values of u_{Li} and u_K thus obtained from these data are plotted in Figure 4a in comparison with the present ones. The values are in good agreement with ours except for u_K at low x_K (= 0.0323). The Klemm method used in the present study is superior to the Hittorf method used by Moynihan and Laity[16] in terms of the accuracy, since in the former the mobility difference of two species is effectively accumulated around the electrodes.

Table 2. Internal Mobilities at about 913 K Evaluated from the Data Presented by Moynihan and Laity[16]

their run no.	x_K	T^a/K	$Q^{a,b}$	$10^7\ u_{Li}{}^b$ / $m^2 \cdot V^{-1} \cdot s^{-1}$	$10^7\ u_K{}^b$ / $m^2 \cdot V^{-1} \cdot s^{-1}$
1	0.0323	913	-17 ± 1	1.591 ± 0.0005	1.320 ± 0.016
2	0.201	909	0 ± 1	1.191 ± 0.0024	1.191 ± 0.010
4	0.204	912	-1 ± 2	1.188 ± 0.0048	1.176 ± 0.019
5	0.302	911	8 ± 3	1.027 ± 0.0095	1.109 ± 0.021
10	0.496	913	14 ± 2	0.794 ± 0.018	1.008 ± 0.014
12	0.656	918	33 ± 5	0.687 ± 0.028	0.914 ± 0.010
13	0.662	915	39 ± 4	0.663 ± 0.022	0.922 ± 0.007

[a] Although the Q values are given at these temperatures,[16] u_{Li} and u_K given here are estimated at 913 K according to eqs 5 and 6 under the assumption that these Q's are practically equal to those at 913 K. [b] The origin of $\pm$ for Q is not clearly defined in ref 16; thus, it seems that the meaning of $\pm$ for u_{Li} or u_K is not necessarily equal to that given in Table 1.

Other data presented by two groups[18,19] were measured by the Klemm method; however, these data cannot be directly compared with the ones in the present study, as the temperature range is lower[18] and the concentration range limited.[19]

Smirnov et al.[17] reported the (external) transport numbers at 1100 K, estimated by the emf method. From their data, the internal mobilities of Li^+ and K^+ can be obtained from the external transport numbers. It has previously been discussed, however, that the emf method cannot, in principle, give accurate values for the internal mobilities, particularly for a cation at a low concentration in a binary mixture with a common anion.[20] Furthermore, since their data on the external transport numbers are shown only graphically as a function of x_K, the internal mobilities could not be calculated precisely. These data are therefore not taken into account here.

4.2. Application of the Empirical Equation. An empirical equation has previously been presented[11,28] on the basis of the data on internal mobilities of 10 binary alkali nitrate systems:

$$u_M = [A_M/(V_m - V_{0M})]\exp(-E_M/RT) \quad (9)$$

where V_m is the molar volume, T the temperature, E_M the activation energy, and R the gas constant. A_M and V_{0M} are constants which depend on the cation M^+; they are nearly independent of the temperature at lower temperatures. We call V_{0M} the deviation (molar) volume here; it will be discussed in 4.4.

From eq 9, it follows:

$$1/u_M = a_M V_m - b_M \quad (10)$$

where

$$a_M \equiv (1/A_M)\exp(E_M/RT) \quad (11)$$

$$b_M \equiv (V_{0M}/A_M)\exp(E_M/RT) \quad (12)$$

To see the validity of eq 9 for the present case, we plot the values of $u_M{}^{-1}$ ($M = Li^+$ and K^+) against the molar volume, V_m, at (913 and 973) K in Figure 5. At 913 K, one straight line is drawn for Li^+, whereas straight lines with two different slopes are drawn for K^+. On the other hand, at 973 K, two straight lines can be drawn both for Li^+ and K^+. As for K^+, it is not clear whether or not, at a higher range of V_m, there exists another straight line with a smaller slope, because the estimated conductivity for the imaginary supercooled KCl melt is not reliable, particularly at the lower temperature, 913 K. In the following, we presume that there are only two ranges with different slopes at (913 and 973) K for K^+.

From eq 9, we get

$$u_M(V_m - V_{0M}) = A_M \exp(-E_M/RT) \quad (13)$$

Here, we define C_{IM} and C_{IIM} by

$$C_{IM} \equiv u_M(V_m - V_{0M}) \quad (14)$$

$$C_{IIM} \equiv A_M \exp(-E_M/RT) \quad (15)$$

Then, it follows from eqs 11, 13, 14, and 15 that

$$C_{IM}\ (=C_{IIM}) = 1/a_M \quad (16)$$

The C_{IM} versus V_m plot according to eq 14 will show the validity of eq 9 more explicitly than the slope, a_M, does. Thus, C_{IM} is plotted against V_m in Figure 6. The values of C_{IM} and V_{0M} can be calculated by a least-squares fit[9,10] for the ranges where the slopes a_M are constant in Figure 5, since the values of u_M and V_m used in eq 14 are available from experiments at more than two points. The values of C_{IM} are also given in Table 3. In spite of eq 16, the values of C_{IM} in Table 3 are not exactly equal to the corresponding values of $1/a_M$ because the weights for the least-squares fits are different. The former is more meaningful as a linear function of the internal mobility, as eq 14 shows. On the other hand, the expression of the reciprocal mobility is indispensable for estimating the reflection point (RP) of the mobility, as shown in Figure 5. Both Figures 5 and 6 are useful also for checking how accurate each data point on u_M is, which is not clear from Figure 4 alone.

It is interesting to note that, according to the molecular dynamics (MD) results for the present system by Morgan and Madden,[29] the calculated $1/u_K$ plotted against the molar volume seems to have RPs at (1096 and 1000) K (cf. Figure 8 in ref

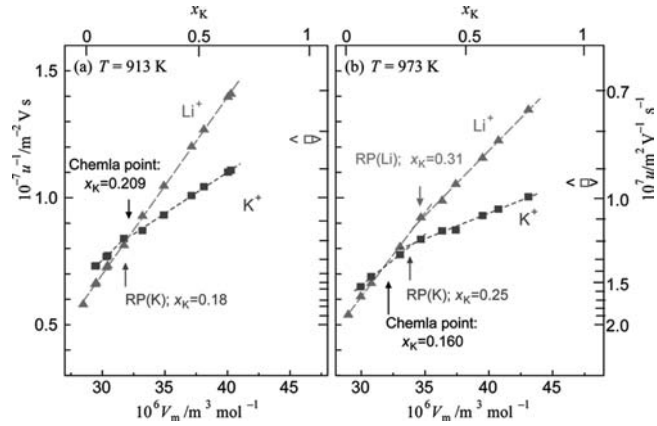

Figure 5. Reciprocal internal mobilities vs the molar volume at 913 K (a) and 973 K (b). RP, reflection point; <□>, see the footnote of Figure 4.

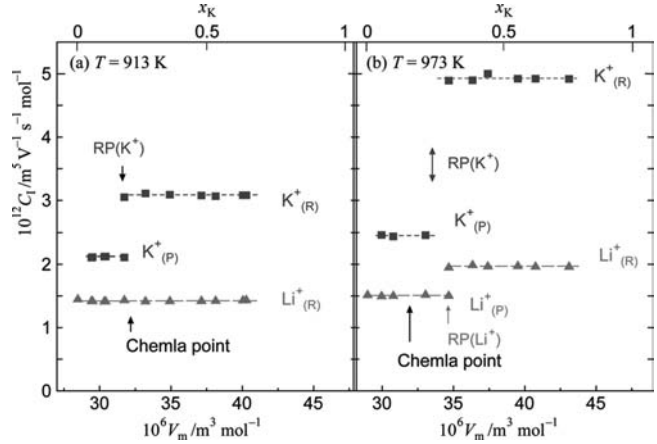

Figure 6. C_I [$\equiv u_M(V_m - V_{0M})$] vs V_m at 913 K (a) and 973 K (b). RP, reflection point; (R), regular mode; (P), perturbed mode.

Table 3. Calculated Values of C_I, V_0, a, and b in the R-Mode and the P-Mode

T			$10^6\ V_m$ / $m^3 \cdot mol^{-1}$		$10^{12}\ C_I$	$10^6\ V_0$	$10^{-11}\ a$	$10^{-6}\ b$
K	M	mode[a]	low	high	$m^5 \cdot V^{-1} \cdot s^{-1} \cdot mol^{-1}$	$m^3 \cdot mol^{-1}$	$m^{-5} \cdot V \cdot s \cdot mol$	$m^{-2} \cdot V \cdot s$
913	Li^+	R	28.5	40.3[b]	1.422 ± 0.012	20.09 ± 0.10	6.982 ± 0.043	13.95 ± 0.14
	K^+	P	29.4	31.7; $x_{Li} = 1$ to 0.82[c]	2.115 ± 0.095	14.02 ± 0.73	4.734 ± 0.172	6.65 ± 0.52
	K^+	R	31.7	40.3[b]	3.080 ± 0.082	6.11 ± 0.80	3.245 ± 0.071	1.98 ± 0.07
973	Li^+	P	29.0	34.7; $x_{Li} = 1$ to 0.69[c]	1.505 ± 0.029	20.82 ± 0.19	6.690 ± 0.101	13.79 ± 0.32
	Li^+	R	34.7	43.1[b]	1.965 ± 0.052	16.71 ± 0.57	5.108 ± 0.103	8.58 ± 0.40
	K^+	P	30.0	33.7; $x_{Li} = 1$ to 0.75[c]	2.455 ± 0.273	13.95 ± 1.91	4.039 ± 0.231	5.57 ± 0.72
	K^+	R	33.7	43.1[b]	4.926 ± 0.331	-6.27 ± 3.00	2.013 ± 0.112	-1.34 ± 0.44

[a] R: regular mode, P: perturbed mode. [b] Upper range for the measurement. [c] Mole fraction of Li^+ in the perturbed mode; the sign $\pm$ designates the standard deviation in the least-squares fit.

29), although the ratio of the slopes below and above the RP at 900 K appears to be opposite to that at (1096 and 1000) K and to the present experimental results.

Figures 5 and 6 and Table 3 lead to the following conclusions: For Li^+,

(i) At the lower temperature ($T = 913$ K), C_{ILi} is constant in the investigated concentration range and in the "regular mode".

(ii) At the higher temperature ($T = 973$ K), C_{ILi} has two different values: (ii-1) At a higher molar volume ($V_m \geq 34.7$ $cm^3 \cdot mol^{-1}$: $x_K \geq 0.31$) C_{ILi} is constant and seems to be in the "regular mode", as at the lower temperature (see (i)). (ii-2) At the lower molar volume ($V_m \leq 34.7$ $cm^3 \cdot mol^{-1}$), that is, at the high concentration of Li^+ ($x_{Li} > \sim 0.7$), C_{ILi} is also constant, but the value is lower than that mentioned above in (ii-1). This is due to the higher value of V_{0Li} (than that in (ii-1)). The lower value of C_I than in (ii-1) is considered to be due to behavior in the "perturbed mode".

For K^+, both at $T = 913$ K and $T = 973$ K;

(iii) Two ranges are observed, and the molar volume of the RP in Figure 5 is $V_m = 31.7$ $cm^3 \cdot mol^{-1}$ ($x_K = 0.18$) at 913 K and 33.7 $cm^3 \cdot mol^{-1}$ ($x_K = 0.25$) at 973 K, as given in Table 3. The regular mode and the perturbed mode will be discussed in Sections 4.3, 4.4, and 4.5.

From the values of C_I and V_0 in Table 3, the molar volume at the Chemla point can be derived by putting $u_{Li} = u_K$ in eq 14 for Li^+ and K^+:

$$V_m(\text{Chemla point}) = (C_{IK}V_{0Li} - C_{ILi}V_{0K})/(C_{IK} - C_{ILi}) \quad (17)$$

The molar volumes at the Chemla point are calculated to be 32.1 $cm^3 \cdot mol^{-1}$ (regular mode for both cations) and 31.7 $cm^3 \cdot mol^{-1}$ (perturbed mode for both cations) at (913 and 973) K, respectively. These values (32.1 $cm^3 \cdot mol^{-1}$ at 913 K and 31.7 $cm^3 \cdot mol^{-1}$ at 973 K) are in good agreement with the values (32.2 $cm^3 \cdot mol^{-1}$ at 913 K and 32.0 $cm^3 \cdot mol^{-1}$ at 973 K, as stated in the Section 3, Results) obtained from Figure 4. This agreement also indicates that the values of C_I and V_0 given in Table 3 are accurate enough.

The Chemla point does not explicitly appear in the C_I values. Phenomenologically, the Chemla effect occurs owing to the fact that $V_{0Li} \gg V_{0K}$. While at a lower V_m, one has $(V_m - V_{0Li}) \ll (V_m - V_{0K})$; at higher V_m the relative difference becomes smaller. Thus, u_{Li} may become smaller than u_K above a certain V_m (at the Chemla point) under the condition that both C_{ILi} $\{= u_{Li}(V_m - V_{0Li})\}$ and C_{IK} $\{= u_K(V_m - V_{0K})\}$ are constant, where $C_{ILi} < C_{IK}$.

4.3. Temperature Dependence. In previous work,[19] the internal mobilities were investigated at $x_K = 0.440$ in a wide temperature range. In the present work, they are measured in a wide concentration range at (913 and 973) K. The common logarithms of the internal mobilities, u_{Li} and u_K, at $x_K = 0.440$ are plotted against the reciprocal temperature in Figure 7.

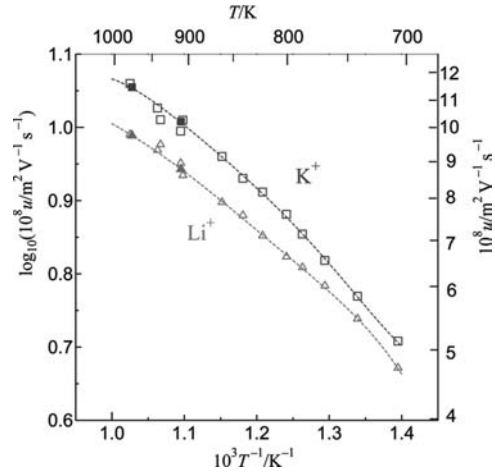

Figure 7. Common logarithms of the internal mobility at $x_K = 0.440$ vs the reciprocal temperature. ▲, ■, this work; △, □, Lundén and Okada.[19]

Figure 7 reveals that the logarithms of u_M against $(1/T)$ are not straight lines but that $d^2(\log_{10} u_M)/d(1/T)^2$ is slightly negative. This indicates that the internal mobilities cannot be expressed by a simple Arrhenius-type equation. On the other hand, if eq 15 holds, ln C_{II} (= ln C_I) plotted against $(1/T)$ should be a straight line.

At about 500 °C (773 K), six data points [between (773 and 782) K] on the internal mobilities are available in a relatively extended concentration range, as seen from Figure 1. Thus, the internal mobilities are calculated at 773 K on the assumption that these data on ε[18,19] or Q,[16] which have been measured at temperatures between (773 and 782) K, are the same to those at 773 K. At first, C_{ILi} and C_{IK} were calculated with a least-squares fit. C_{IK} is then recalculated for four data points excluding the other two data points having significanly larger values (as shown in Figure 8). The values of V_0 can be calculated at the same time. The resulting C_I values are plotted versus the molar volume in Figure 8.

In Figure 9, the natural logarithms of C_I thus obtained are plotted against $(1/T)$. The logarithms of C_{ILi} and C_{IK} at 773 K and those at (913 and 973) K, which are presumed to correspond to a regular mode, lie on straight lines.

This supports the assumption that C_{ILi} and C_{IK} in the regular mode are well-expressed by eq 13; the A and E are calculated by least-squares fits of an exponential form and given in Table 4. The E_K is clearly larger than E_{Li}, as is in (Li, K)Br.

Figure 9 shows that the C_I(P), which is ascribed to the perturbed mode, deviates considerably from that corresponding to the regular mode, C_I(R), for Li^+ at 973 K and for K^+ at (913

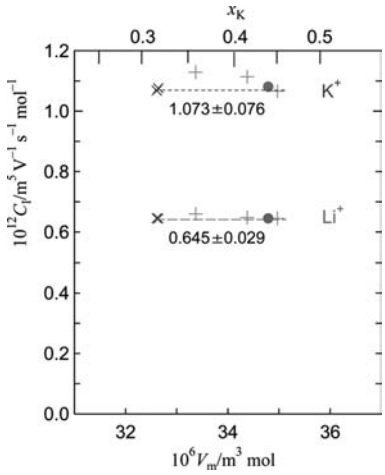

Figure 8. C_I values estimated at 773 K vs the molar volume. For the marks, see the footnote of Figure 1. The values given are calculated from six data points for Li^+ and four data points for K^+; two high values of (+) for K^+ are omitted for calculation of the average C_I. The sign ± indicates the standard deviation.

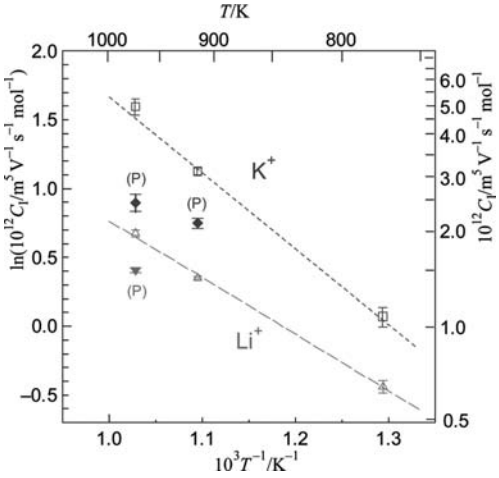

Figure 9. Natural logarithms of C_I vs $1/T$. △, □, C_{ILi} and C_{IK}, respectively, in the regular mode at (913 and 973) K (this work) and at 773 K (calculated from the previously obtained data[16,18,19]); ▼, ◆, C_{ILi} and C_{IK}, respectively, in the perturbed mode.

Table 4. Parameters *A* and *E* in C_{II} in Equation 15

system	temp. range[a]	M	$10^{11}\,A$ / $m^5\cdot V^{-1}\cdot s^{-1}$	E / $kJ\cdot mol^{-1}$	ref
chloride	(773 to 973) K	Li^+	13.9 ± 5.2	34.8 ± 2.9	this work
		K^+	134.0 ±71.0	46.0 ± 4.0	
bromide	(633 to 923) K	Li^+	2.14	20.0	refs 9, 10
		K^+	7.78	26.1	
	(923 to 1023) K	Li^+	4.51	25.8	
		K^+	143.2	48.7	

[a] The temperature range where the parameters *A* and *E* are obtained. The sign ± designates the standard deviation in the least-squares fit of an exponential form.

and 973) K. As the temperature range of the data is limited, the temperature dependence is not calculated. The deviation becomes larger with temperature. Figure 9 demonstrates which of the two modes corresponds to the regular mode, which is not clear from Figure 6 alone.

With these C_I values, V_0 can be obtained from eq 14 from the available data on u_M at $x_K = 0.440$. The calculated values of V_0 are shown as a function of $1/T$ in Figure 10 along with those in the bromide system.[9,10]

From eqs 11, 12, and 15, it follows:

$$V_0 = (b/a) = bA\exp(-E/RT) \tag{18}$$

Here, b is also temperature-dependent, because $-b$ is the intercept of the linear function of $1/u$ ($= aV_m - b$: eq 10). $-b_M$ increases with increasing temperature, and therefore b_M decreases, as can be seen also from Figure 5. The decrease in V_0 with increasing temperature (Figure 10) indicates that, as temperature increases, b overcompensates the term $\exp(-E/RT)$ in eq 18. It is also understandable from the standpoint of eq 18 that V_{0K} possesses even negative values at high temperature, because b_M could become negative.[9]

4.4. Deviation Volume, V_0. In the dynamic dissociation model,[30] the local number density of common anions is considered to play an important role in the mobility, as it will be seen in Section 4.5. If the anions were uniformly distributed, their number density would be N_A/V_m; N_A is Avogadro's number. However, as the local number density must deviate from the bulk one, this may be proportional to $1/(V_m - V_0)$, where V_0 is regarded as a deviation volume characteristic of a cation of interest.

From the viewpoint of the structure, the significance of the V_0 value is roughly this; $(V_m - V_0)$ can be regarded as the local molar volume of the common anion. As seen from Figure 10, V_0 seems to attain a constant value with decreasing temperature; this trend is particularly clear for Li^+. At a low temperature, V_0 may be considered to be nearly independent of the cation concentration.

Figure 10 shows that the decrease in V_0 with increasing temperature is more moderate for Li^+ than for K^+ and in the bromide than in the chloride. These would imply that, as the cation/anion radius ratio is smaller, the local structure is more stable with respect to an increase in temperature. In other words, the large change in V_0 for K, accompanied by a temperature increase, will lead to a significant change in the local structure.

The large difference between the two systems is that in the chloride system V_0 in the perturbed mode appears at a higher temperature and in a higher x_{Li} range than the RP (see also Figure 5). V_{0Li} and V_{0K} in the perturbed mode are larger than the corresponding ones in the regular mode; that is, the value of $(V_m - V_0)$ becomes smaller when the concentration of Li^+ is high. This is presumably because at high temperatures the ions are more associated at high concentrations of Li^+; the local coordination number around a cation would thus change

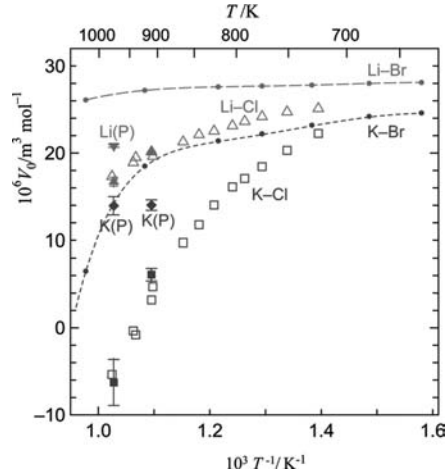

Figure 10. Estimated V_0 at $x_K = 0.44$ vs $1/T$. ▲, ■, V_{0Li}, V_{0K}, respectively, in the regular mode; ▼, ◆, V_{0Li}, V_{0K}, respectively, in the perturbed mode; △, □, V_{0Li}, V_{0K}, respectively, calculated from ref 19; −−●−−, --●--, V_{0Li}, V_{0K}, respectively, for the bromide at $x_K = 0.40$.[10]

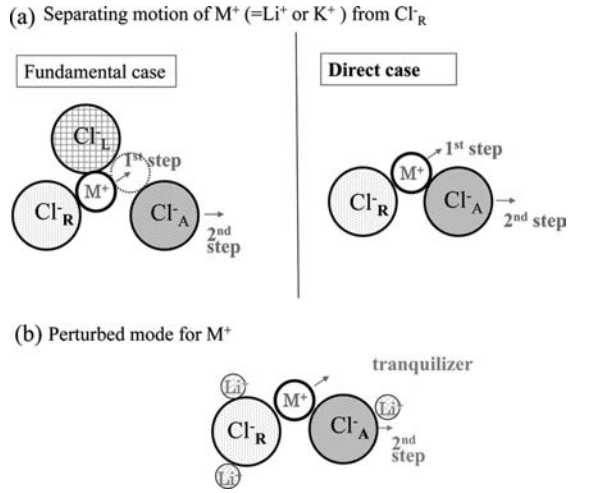

Figure 11. Schematic diagrams of separating motion of M^+ (= Li^+ or K^+) from its reference anion (Cl^-_R) toward the neighboring attracting Cl^- (Cl^-_A). (a) Fundamental case: leading anion (Cl^-_L) helps the motion of M^+ toward Cl^-_A; and direct case; (b) perturbed mode.

unsmoothly at the RP. However, the existence of the RP has not so far been observed in other properties such as the structure.

4.5. Dynamic Dissociation Model. The observations mentioned in (i) to (iii) in Section 4.2 can, qualitatively, be accounted for in terms of the dynamic dissociation model;[30] it is assumed that the internal mobility of a cation is strongly related with the separating motion from its reference anion, as schematically shown in Figure 11a.

It has been previously analyzed by MD simulations for the separating motion of several individual cations from their reference Cl^- ion in the present system ($x_K = 0.417$).[31] A cation oscillates around the reference anion during an extended time and then suddenly moves away, although in some occasions it may come back soon. These motions have been classified into the oscillating process (O-process), the leaving-process (L-process), and the coming-back process (C-process), respectively. It is noteworthy that the velocity of the L-process depends only on the temperature and the masses of the two relevant ions and is independent of the kind of other coexisting ions. In other words, the L-process seems to proceed without surmounting a potential barrier. The average velocity of the separating motion is determined mainly by the frequency of the occurrence of the L-process, in other words, by the duration of the O-process; the average velocity has been named the self-exchange velocity (SEV),[32] which has been found to be closely correlated with the (experimentally measured and calculated) internal mobility.[29,31,32]

Since, in Figure 11, the Coulombic interaction between the cation, M^+, and the reference anion, Cl^-_R, is so strong, the M^+ cannot move away from Cl^-_R because of the kinetic energy alone without the presence of another attracting anion. Therefore, in the dynamic dissociation model the role of the attracting anion is regarded as essential.

In the case referred to as the fundamental case, a "leading" anion, Cl^-_L, can transport the M^+ to a Cl^-_A without surmounting the Coulombic potential barrier, and then Cl^-_A would leave together with the M^+ from Cl^-_R. Under some conditions, such as high temperature and large free space, Cl^-_A can separate M^+ from Cl^-_R without the help of Cl^-_L; this is referred to as the direct case in Figure 11a. This case would rarely occur at low temperatures and small free space, because M^+ would immediately return back to the Cl^-_R by the O-process or by the C-process.

In the region for the perturbed mode, C_I values are smaller than those for the regular mode (see Figure 6). The perturbed mode occurs in the following cases: for Li^+, at a higher concentration of Li^+ when the temperature is high (973 K), and for K^+, at a higher concentration of Li^+ at both the low temperature and the high temperature. For K^+, the concentration range of Li^+ for the perturbed mode becomes wider at a higher temperature ($x_{Li} > 0.82$ at 913 K and $x_{Li} > 0.75$ at 973 K, as given in Table 3). These findings suggest that the perturbed mode is due to the tranquilization effect[11] caused by the strongly associated Li^+ ions with the attracting Cl^- and the reference Cl^-, which is schematically shown in Figure 11b.

The present system (Li, K)Cl is the first case analyzed for the perturbed mode in terms of the C_I value; in the system (Li, K)Br previously analyzed,[9,10] the perturbed mode does not occur. A similar analysis is thus needed for other binary alkali chlorides and bromides for further explanations of the perturbed mode.

4.6. Comparison with (Li, K)Br. It has been found[9,10] that the binary system (Li, K)Br containing a trace amount of radioactive Na^+, investigated by Chemla's group,[5−7] can be regarded as an "ideal system" in the sense that C_{ILi}, C_{IK}, and even C_{INa} for Na^+ are constant over the whole investigated concentration range, both in the lower temperature range (below 923 K) and at a higher temperature (1023 K), except for one case: the C_{IK} in pure LiBr (radioisotope ^{42}K was used[5]) at 1023 K is significantly higher than that at the other concentrations.[9,10] This has been attributed to the agitation effect[11] by the abundant Li^+ ions; we assume that this effect overcomes the tranquilization effect. This is in contrast with the present case, probably because the mass of Br^-_A as the attracting anion is too large compared with that of the tranquilizer Li^+ (see Figure 11b), and the second step of Br^- (see Figure 11b) will not be retarded as much by the cohesive tranquilizer.

As for the temperature dependence of C_I in the regular mode in (Li, K)Br, C_I at a higher temperature (1023 K) is significantly higher, particularly for K^+, than that expressed by C_{II} (= $A \exp(-E/RT)$) with the E at a lower temperature as given in Table 4. Also in the present system, the C_{IK} at 973 K seems to be slightly higher than C_{IIK}, expressed with the parameter E at the lower temperature, as seen from Figure 9. Thus, E_K seems to be positively temperature-dependent at higher temperatures in both systems, whereas E_K is constant at lower temperatures. Meanwhile, the temperature dependence of E_{Li} is still relatively small for the investigated temperatures of the present system.

A difference between the present system and the bromide system is that in the former the RP appears in a plot of $(1/u)$ versus V_m, whereas in the latter no RP appears in the range from (633 to 1023) K. This is presumably because, in the bromide system, the structure inside the coordination shell around the cations does not change much because of the large size of Br^- in comparison with the cations and its large mass.

5. Conclusions

The internal mobilities in the molten system (Li, K)Cl have been measured in a wide range of concentration at (913 and 973) K. These are compared, where possible, with those previously reported. The present results at 913 K are in good agreement with those obtained by Moynihan and Laity, except for a value at high molar fraction x_{Li}. The results are analyzed in a new approach.

The C_I value defined by the product of the internal mobility and the modified molar volume is found to have two different values, depending on the concentration range, at (913 and 973) K, except for C_{ILi} at 913 K which has one single constant value over

the whole investigated concentration range. C_{IK} is always larger than C_{ILi} at the investigated temperatures, and no crossing occurs.

(I) In the entire investigated concentration range at 913 K and in the lower x_{Li} range at 973 K, u_{Li} is classified as being in the regular mode, because C_I can be expressed by $C_I = A \exp(-E/RT)$ from 773 K through 973 K.

(II) At 973 K and at a high x_{Li}, u_{Li} belongs to the perturbed mode. C_{ILi} is constant also in this range; it cannot be expressed by a form of $C_I = A \exp(-E/RT)$ with E evaluated at a lower temperature, whereas C_I (perturbed mode) < C_I (regular mode), V_0 (perturbed mode) > V_0 (regular mode).

(III) u_K at (913 and 973) K in the low x_{Li} range is classified as being in the regular mode.

(IV) u_K at these temperatures, but in the high x_{Li} range, is associated to the perturbed mode, caused by the tranquilization effect by Li^+.

The change in C_{IM} from one value to another, at a given temperature, seems to occur nearly discontinuously around a certain molar volume; this point is named the RP of the internal mobility. The molar volumes at the RP are different for Li^+ and K^+ and dependent on the temperature. They are thus different from those of the Chemla crossing point. The Chemla effect occurs irrespective of being in the regular mode or the perturbed mode.

The internal mobilities for (Li, K)Cl are in contrast with those of (Li, K)Br previously analyzed in that the latter mixture system shows a regular mode nearly in the whole investigated concentration and temperature range.

In summary, the internal cation mobilities in the present system seem to follow the regular mode only if the coordination structure around the cation is relatively stable, which occurs when the size ratio of the cation to anion is small and/or the temperature low. When this condition is not fulfilled, the perturbed mode prevails. The dynamic dissociation model seems to hold well for the mobilities, not only in the regular mode but also in the perturbed mode.

Literature Cited

(1) Chemla, M. Improvement of the Isotope Separation Processes by Countercurrent Electromigration in the Molten Salts. (Perfectionnement aux procédés de séparation isotopique par électromigration en contre-courant dans les sels fondus). French Patent No. 1,216,418, Demanded on Nov 24, 1958, 1−2.

(2) Klemm, A.; Hintenberger, H.; Hoernes, P. Enrichment of Heavier Isotopes of Li and K by Electromigration in Molten Chlorides. (Anreicherung der Schweren Isotope von Li und K durch Electrolytische Ionenwanderung in Geschmolzenen Chloriden). *Z. Naturforsch.* **1947**, *2a*, 245–249.

(3) Périé, J.; Chemla, M. Countercurrent Electromigration in Molten Halide Mixtures. (Électromigration en Contre-courant dans des Mélanges d'Halogénures Fondus. *C. R. Acad. Sci.* **1960**, *250*, 3986–3988.

(4) Périé, J.; Chemla, M.; Gignoux, M. Separation of Isotopes by Countercurrent Electromigration in Molten Alkali Bromides. (Séparation d'Isotopes par Électromigration en Contre-courant dans des Systèmes d'Halogénures Fondus). *Bull. Soc. Chim. Fr.* **1961**, 1249–1256.

(5) Mehta, O. P. Study on Ion Transport in Molten Alkali Bromides. (Étude du Transport Ionique dans des Bromures Alcalins Fondus). Thesis, Faculté des Science, Université d'Orsay, France, 1967.

(6) Mehta, O. P.; Lantelme, F.; Chemla, M. Electric Conductivity of the Molten Systems LiBr−KBr. (Conductibilité Électrique des Systèmes LiBr-KBr Fondus). *Electrochim. Acta* **1969**, *14*, 505–513.

(7) Chemla, M.; Lantelme, F.; Mehta, O. P. Diffusion and Transport in Molten Alkali Halides. (Diffusion et Transport Ionique dans les Halogénures Alcalins Fondus). *J. Chim. Phys. (Num. Spec.)* **1969**, 136–144.

(8) Okada, I.; Takagi, R.; Kawamura, K. Internal Cation Mobilities in the Molten System (Li-Rb)NO_3 and (Li-Cs)NO_3. *Z. Naturforsch.* **1979**, *34a*, 498–503.

(9) Okada, I.; Lantelme, F. A New Interpretation of the Original Data of Chemla's Group on the Mobilities of Binary Molten System (Li, K)Br. *J. New Mater. Electrochem. Syst.* **2006**, *9*, 165–174.

(10) Okada, I.; Lantelme, F. Application of an Empirical Internal Mobility Equation to the Molten Binary Bromide System (Li, K)Br Studied by Chemla's Group. *Z. Naturforsch.* **2008**, *63a*, 318–320.

(11) Chemla, M.; Okada, I. Ionic Mobilities of Monovalent Cations in Molten Salt Mixtures. *Electrochim. Acta* **1990**, *35*, 1761–1776.

(12) Okada, I. Transport Properties of Molten Salts. In *Modern Aspects of Electrochemistry*, Number 34; Bockris, J. O'M., Ed.; Kluwer Academic/Plenum Publishers: New York, 2001; pp 119−203.

(13) Okada, I. The Chemla Effect-from the Separation of Isotopes to the Modeling of Binary Ionic Liquids. *J. Mol. Liq.* **1999**, *83*, 5–22.

(14) Okada, I. Electric Conduction in Molten Salts. *Electrochemistry (Tokyo, Jpn.)* **1999**, *67*, 529–540.

(15) Janz, G. J.; Tomkins, R. P. T.; Allen, C. B.; Downey, J. R., Jr.; Gardner, G. L.; Krebs, U.; Singer, S. K. Chlorides and Mixtures Electrical Conductance, Density, Viscosity, and Surface Tension Data. *J. Phys. Chem. Ref. Data* **1975**, *4*, 871–1178.

(16) Moynihan, C. T.; Laity, R. W. Relative Cation Mobilities in Potassium Chloride-Lithium Chloride Melts. *J. Phys. Chem.* **1964**, *68*, 3312–3317.

(17) Smirnov, M. V.; Alexandrov, K. A.; Khokhlov, V. A. Diffusion Potentials and Transport Numbers in Molten Alkali Chlorides and Their Binary Mixtures. *Electrochim. Acta* **1977**, *22*, 543–550.

(18) Takagi, R.; Shimotake, H.; Jensen, K. J. Determination of Internal Cation Mobilities in the Molten System (Li-K)Cl at 273 K. *J. Electrochem. Soc.* **1984**, *131*, 1280–1283.

(19) Lundén, A.; Okada, I. Internal Cation Mobilities and their Isotope Effects in the Molten System (Li, K)Cl. *Z. Naturforsch.* **1986**, *41a*, 1034–1040.

(20) Ichioka, K.; Okada, I.; Klemm, A. Internal Cation Mobilities in Molten (Na, Ag)NO_3 Remeasured by the Column Method. *Z. Naturforsch.* **1989**, *44a*, 747–750.

(21) Ljubimov, V.; Lundén, A. Electromigration in Molten and Solid Binary Sulfate Mixtures: Relative Cation Mobilities and Transport Numbers. *Z. Naturforsch.* **1966**, *21a*, 1592–1600.

(22) Okada, I.; Horinouchi, H. The Chemla Effect in the Mobilities in the Molten Binary System of Lithium Chloride and Caesium Chloride. *J. Electroanal. Chem.* **1995**, *396*, 547–552.

(23) Van Artsdalen, E. R.; Yaffe, I. S. Electrical Conductance and Density of Molten Salt Systems: KCl-LiCl, KCl-NaCl and KCl-KI. *J. Phys. Chem.* **1955**, *59*, 118–128.

(24) Janz, G. J. Thermodynamic and Transport Properties for Molten Salts: Correlation Equations for Critically Evaluated Density, Surface Tension, Electrical Conductance, and Viscosity Data. *J. Phys. Chem. Ref. Data, Suppl.* **1988**, *17*, 1–309.

(25) Fellner, P.; Votava, I.; Chrenková-Paučírová, M. Density of the Molten System LiCl-NaCl-KCl. *Chem. Zvesti* **1980**, *34*, 330–334.

(26) Fellner, P. The Series and Parallel Models of Electrical Conductivity of Molten Salt Mixtures. I. Binary Mixtures with Simple Halide Anions. *Chem. Zvesti* **1984**, *38*, 159–163.

(27) Daněk, V. Dissociation Model of the Electrical Conductivity of Molten Salt Mixtures I. Theory of Univalent Electrolytes. *Chem. Pap.* **1989**, *43*, 25–34.

(28) Yang, C.-C.; Takagi, R.; Okada, I. Internal Cation Mobilities in the Molten Systems (Li-Na)NO_3 and (Na-Cs)NO_3. *Z. Naturforsch.* **1980**, *35a*, 1186–1191.

(29) Morgan, B.; Madden, P. A. Ionic Mobilities and Microscopic Dynamics in Liquid (Li, K)Cl. *J. Chem. Phys.* **2004**, *120*, 1402–1413.

(30) Koura, T.; Matsuura, H.; Okada, I. A Dynamic Dissociation Model for Internal Mobilities in Molten Alkali and Alkaline Earth Nitrate Mixtures. *J. Mol. Liq.* **1997**, *73−74*, 195–208.

(31) Okada, I. MD-Simulation of Molten (Li, K)Cl at the Eutectic Composition. Self-Exchange Velocities of Li- and K-Isotopes near the Cl^- Ions. *Z. Naturforsch.* **1987**, *42a*, 21–28.

(32) Okada, I.; Takagi, R.; Kawamura, K. A Molecular Dynamics Simulation of Molten (Li-Rb)Cl Implying the Chemla Effect of Mobilities. *Z. Naturforsch.* **1980**, *35a*, 493–499.

Received for review October 21, 2009. Accepted February 5, 2010.

JE900866Q